# Accurate Vehicle Positioning on a Numerical Map

## Jean Laneurit, Roland Chapuis, and Frédéric Chausse

**Abstract:** Nowadays, the road safety is an important research field. One of the principal research topics in this field is the vehicle localization in the road network. This article presents an approach of multisensor fusion able to locate a vehicle with a decimeter precision. The different informations used in this method come from the following sensors: a low cost GPS, a numeric camera, an odometer and a steer angle sensor. Taking into account a complete model of errors on GPS data (bias on position and nonwhite errors) as well as the data provided by an original approach coupling a vision algorithm with a precise numerical map allow us to get this precision.

**Keywords:** Multisensor fusion , Kalman filter, GPS, artificial vision.

## 1. INTRODUCTION

Developing systems to improve driving security has become a major research field in recent years. There are many international projects such as PROMETHEUS[1], ROADSENSE[2] and french national project in the framework of the PREDIT program like PAROTO[3] and ARCOS[4]. One important purpose of the embedded systems is to localize a vehicle in the road network (GPS/Map navigation system). However, if the system has to provide an active control of the vehicle (automatic cruise control, automatic lightning control, collision avoidance, ...), localization becomes unavoidable. The localization must be precise and robust. Differential GPS is to provide a sufficient accuracy (about one centimeter) but this system has major drawbacks :

- a fixed transceiver must be used in addition to the on-boarded mobile GPS receiver,
- the cost is prohibitive for a wide scale public marketing,
- it is very sensitive to satellite occlusions (due to buildings, bridges, ...).

We have designed a system able to avoid these disadvantages. It provides localization information with an accuracy of about $10cm$. It is a low cost system and easy to load on board which is also rather insensitive to GPS data losses. Our system is constituted of the original association of :

- an image processing algorithm giving precisely the lateral position and the orientation of the vehicle with reference to the road sides (local positioning),
- a low cost, low precision GPS,
- proprioceptive sensors (odometer, steer angle) to predict the vehicle motion,
- an accurate numerical map of the road network.

This method is fully described in this article. The bibliography of the first section underlines the frequent use of GPS for vehicle localization and specifies systematically that GPS are subject to a bias and are perturbed by a non white noise with normal PDF. These well known characteristics of GPS data are commonly neglected and the error is considered as a white noise. We have observed this last assumption leads to a serious decrease of the accuracy. This article proposes a solution to solve that problem by estimating the bias in the same process as the localization parameters. A correct modeling of GPS is necessary : the model we propose is the result of many experiments and constitutes an original aspect of this work. All are explained in the second section.

The third section describes how information provided from image analysis is included in cooperation with a numerical map. The vision/map coupling presented in this section makes it possible to convert the local

information calculated by the vision algorithm into global world reference. The information provided by the vision system being very precise (better than 10cm for the lateral position), the system is able to reach the desired precision.

The estimation of localization parameters necessitates a prediction step and its description is in the fourth section. Finally, the fifth section presents the experimental results showing the validity of the method.

## 1.1. Classification of vehicle localization methods

The numerous methods designed to localize a vehicle or a robot in its environment are often classified into three categories: relative localization, absolute localization and hybrid localization.

### 1.1.1 Relative localization

In a relative localization [4,8,24], the position and orientation of a vehicle are obtained taking into account its successive displacements from a known starting position: travel distance, speed, acceleration, gyration angle. These systems estimate the vehicle's position quickly and frequently. This is why they are often chosen for mobile robots in military or spatial applications. Relative localization is cheap and easy to use. Unfortunately, the derivation of the estimation during time is a main drawback.

### 1.1.2 Absolute localization

This method determines the position of a vehicle or a robot in its environment (indoor or outdoor). It is based on the use of exteroceptive sensors (mainly GPS [14,26]). It can use either natural [15,18] or artificial landmarks [3,23]. The environment has to be known thus a map is necessary [13,20]. There is no derivation of the estimated position during time like with relative localization but the landmarks can become invisible from the robot and the localization is then impossible for a while.

### 1.1.3 Hybrid localization

Both of the localization categories described above use different types of sensors. They provide imperfect measures, which means incomplete, uncertain, and erroneous measures. The comparison (Table 1) of their respective advantages and drawbacks makes their complementarity appear.

In order to palliate their drawbacks and to cumulate their advantages, many systems [3,6], combine the two kinds of methods within a data or multi-sensor fusion framework. The fusion is then made using three types of methods: statistic, probabilistic or grouping methods.

## 1.2. Different methods for data fusion
### 1.2.1 Statistical methods : Kalman filter

Table 1. Comparison relative vs. absolute localization.

| Relative localization | Absolute localization |
|---|---|
| (-) Accumulated error when the distance increases | (+) Error independent of the distance |
| (-) Reference linked to the initial position of vehicle | (+) Absolute world reference |
| (+) No particular equipment in the environ-ment | (-) Environment must sometimes be adapted |
| (+) More frequency use | (-) Less frequency use (-) Possible loss of information |

It is a classical tool for mobile robot [25]. The localization parameters are grouped into a state vector $\underline{X}_k$. The estimation $\widehat{\underline{X}}$ is updated from the former value $\widehat{\underline{X}}_{k-1}$ using proprioceptive sensor data available at time $t_k$. The estimation takes also into account the covariances on the estimation and on the sensor data. If necessary, the equations are linearized around the last estimation. This is the extended Kalman filter [9,12,21] for which two stages are required:

- prediction stage: from the preceding estimation, and according to the values given by proprioceptive sensors and to an equation of evolution, the next value of the state vector is predicted,
- when information from an exteroceptive sensor is available, it is used to correct the predicted state.

A correct estimation will be obtained if the initial position of the vehicle is known with a sufficient accuracy and by knowing the statistical behavior of the data as well as their degree of uncertainty.

### 1.2.2 Probabilistic methods: particles filter

In principle, particles filters [1,17,22] approximate the Probability Density Function (PDF) of the vehicle state $\underline{X}$ from a set of $N$ weighted samples called particles $(\underline{X}_l, \pi_l)$, $\pi_l$ being the weight and $l = 1,...,N$. The process can be divided in three steps:

- re-sampling step: from the the PDF $\mathbf{P}(\underline{X}_{i-1} | z_{i-1})$ ($z_{i-1}$ represents all the data measured up to time $t_{i-1}$) $N$ particles are aleatory drawn, each one receiving a weight equal to $\frac{1}{N}$.
- prediction step: the new position $\underline{X}_{l_{i|i-1}}$ of each sample is predicted from the preceding position using the entries.

- updating step: measures $z_j$ from exteroceptive sensors are taken into account and the weighted becomes $\mathbf{P}(z_j \mid \underline{X}_{l_{j|j-1}})$, namely the probability of observing $z_j$ being positioned on $\underline{X}_{l_{j|j-1}}$. Then the PDF is also updated end becomes $\mathbf{P}(\underline{X}_j \mid z_j)$.

This approach requires no particular knowledge about the initial position of the vehicle: at the beginning, the PDF of the particles are uniformly dispatched among all the possible positions. However, particles filters can manage multi-modal PDFs appearing when uncertain data can lead to several possible solutions. It is an important advantage when systems are highly non linear. The main drawback is the calculation time increasing with the number of particles.

1.2.3 Bounded error methods

These geometric approaches [11,19] are very interesting when no particular hypothesis on the PDF of the measurement errors can be made except for their lower and upper bounds. In particular, errors don't have to be independent or centered. In general, the bounds are provided in the sensor data sheet as an uncertainly interval in which the true value is included with a reasonable probability. Then for a given position of the vehicle, knowing the exteroceptive measures and the magnitude of their respective noise, a system of inequation is set up, the state must be satisfy.

The result is a polyhedron in the state space. It is determined iteratively by intersection of the current polyhedron with the interval corresponding to the current measure. The final polyhedron has a complex shape as the number of facets is not bounded. This is why simple shapes are often used (generally ellipsoids described by a center and a positive matrix) including all the possible values. Several algorithms can help determining the ellipsoids: minimizing the determinant of the matrix associated with the ellipsoid [16] (volume homogeneity) or minimizing the matrix trace corresponding to the sum of the square half-length of the ellipsoids axis.

This method has a main drawback: finding a correct solution is not guaranteed if the measure equations are non linear regarding the state parameters.

1.3. Our approach

According to the classification made in Section 1.1. we propose an hybrid localization method with proprioceptive sensors (odometer, steering angle) and exteroceptive sensors (GPS, camera associated with an image processing algorithm able to detect lane sides) an a pre-loaded numerical map of the environment. The data fusion is achieved using a Kalman filter.

The goal is to estimate the attitude of a vehicle in 2D reference frame of the world (flat earth assumption). The estimation must be precise and must use cheap sensors.

The attitude is represented by the state vector associated with its covariance matrix $\mathbf{Q}_a$.

$$\underline{X}_a = (x, y, \gamma)^t \tag{1}$$

with:

- $x$ abscissa of the position in the world reference,
- $y$ ordinate of the position in the world reference,
- $\gamma$ vehicle orientation angle in the world reference,

and

$$\mathbf{Q}_a = \begin{pmatrix} \sigma_x^2 & \sigma_{xy} & \sigma_{x\gamma} \\ \sigma_{yx} & \sigma_y^2 & \sigma_{y\gamma} \\ \sigma_{\gamma x} & \sigma_{\gamma y} & \sigma_\gamma^2 \end{pmatrix}. \tag{2}$$

The method can be divided into three steps:

- prediction of the vehicle attitude from the last estimation using the proprioceptive data and an equation describing the evolution of the vehicle
- state update using GPS data after their conversion into the chosen frame of reference
- state update from the vision data, the translation of the local information given by the vision algorithm in made using the numerical map.

Data comes from particular sensor at any time. It means all the sensors are not synchronized. The preceding stages can be realized at any times regardless the order presented above. Each step is described in the next sections and localization results obtained in urban area are given.

In addition to the advantages of hybrid solutions already mentioned, the presented method proposes several contributions :
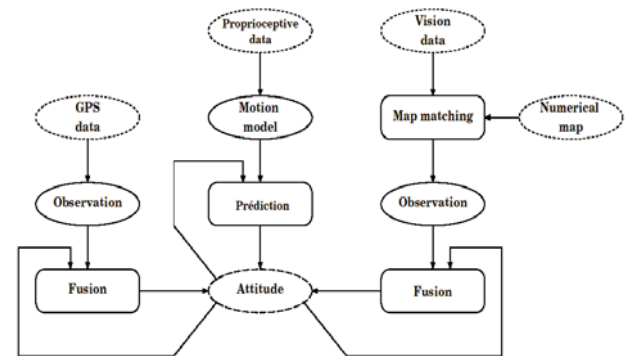


Fig. 1. Localization synoptic.

1. All the other method making use of GPS for precise robot localization utilize differential GPS. These devices are less easy to use (need of a fixed base station or of a subscription to a differential satellite based correction) and above all are very expensive. This make them almost unusable as personal driving assistance systems. On the contrary, our solution is much more cheap.

2. More fundamentally, this article presents a modeling of GPS uncertainties underlying the existence of a bias parameter added to a non white centered low level noise. Most of the time, other methods mention this problem or simply ignore it. The corresponding solutions consider a Gaussian probability density function for GPS uncertainties modeling, overestimating the variance to insure the convergence of the position estimation process. We don't make such approximations. We estimate the bias and take its value into account to compute a more precise GPS position.

3. The main originality of the presented solution rests on the use of a computer vision algorithm able to detect lane sides. Coupled with GPS and a numerical map, it makes it possible to estimate a very precise absolute localization of the vehicle.

## 2. STATE UPDATE BY GPS DATA

### 2.1. GPS system
#### 2.1.1 GPS system description

GPS (Global positioning system) [5] is a localization system based on a constellation of 24 active satellites in orbit around the earth at altitudes of about 20200 km. It provides a position in three dimension and time traceable to global time standards. Theses satellites are arranged in six orbital planes that are inclined at a 55 degree angle, providing worldwide coverage with at least four satellites visible from any point on the earth. Each satellite transmits data frames containing the satellite clock data and orbital data. Range measurement from four satellites are used to compute a receiver clock correction and a three dimensional position.

Two kinds of services are provided by GPS system; SPS (Standard Positioning Service) available to any user and PPS (Precision Positioning Service) reserved for the American government and military users.

#### 2.1.2 Origin of GPS uncertainty

In general three kinds of errors can be distinguished [10] on the range measurement:

- Satellites errors:
  - clock errors,

- satellite ephemeris errors.
- Transmission errors:
  - tropospheric and ionospheric delays,
  - multi-path interferences caused by local reflections of the GPS signal,
  - satellite visibility.
- Receiver noise and delay introduced by its components.

### 2.2. Characteristic of GPS data
#### 2.2.1 Identification

To identify GPS data behavior, GPS coordinates x and y have been acquired during several hours keeping the receiver in a static position. It was positioned near buildings to recreate multi-path interference situations and GPS signal losses. In Fig. 2, graphics 2(a) and 2(b) describe respectively the time evolution of x and y GPS coordinates given by GPS, graphics 2(c) and 2(d) the corresponding histograms measuring the probability density function (PDF) ox x and y considered as random variables. Figs. 2(e) and 2(f) represent the autocorrelation functions of x and y.

For an optimal convergence of Kalman Filter, data distribution must be Gaussian, centered and white. According to histograms 2(c) and 2(d) GPS data can be
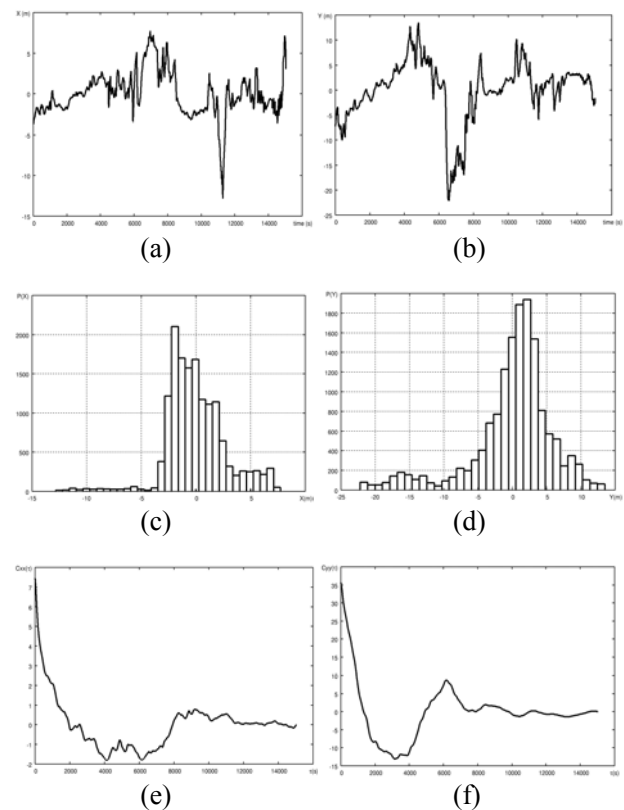


Fig. 2. Characteristics of the GPS data : $x$ and $y$ distributions on graphics (a) end (b), $x$ and $y$ PDFs on graphics (c) and (d), $x$ and $y$ autocorrelation functions of $x$ and $y$ on graphics (e) and (f).

Fig. 3. Variation of GPS data (*x* coordinate).
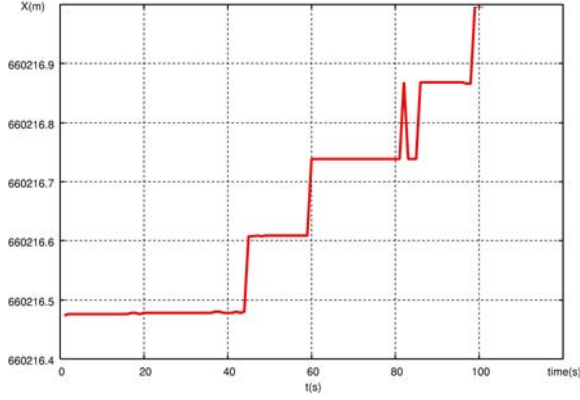


Fig. 4. Modeling of GPS coordinates.

considered as centered and Gaussian with a standard deviation of about 10m. The autocorrelations functions denote a non white frequency spectrum. Therefore GPS data can't feed directly the Kalman filter, a model according to each hypothesis is necessary.

### 2.2.2 GPS data modeling

Glancing at Fig. 3 which is a zoom of Fig. 2(a), the experimental observations underline a step by step time variation of GPS data (remember the receiver is fixed). Anyway, they can be considered as white and centered around a given step.

In addition, when the number of visible satellites changes or when multi-path interferences come upon during the vehicle traveling, data can fluctuate in a strong way but remain in the confidence interval given by the manufacturer.

Therefore the model (Fig. 4) can be described this way: for any position given by GPS, the real vehicle position is equal to GPS position plus a bias $\underline{b} = (b_x, b_y)^t$ plus a white noise $\underline{v}_g = (v_{g_x}, v_{g_y})^t$.

As shown in Fig. 3 the bias $\underline{b}$ will be supposed constant between two GPS data and will be subject to variations smaller than $\Delta_p$ (see Fig. 4). $\Delta_p$ can be described by the following equation:

$$\Delta_P = GDOP \times UERE \tag{3}$$

with:
- *GDOP* : Geometric Dilution of Precision
- *UERE* : User Equivalent Ranging Error.

*UERE* corresponds to the standard deviation of GPS data ($\simeq 10m$). *GDOP* is an integer transmitted on the GPS signal in addition to the position's coordinates.

Taking into account the model of the GPS data, observation for the state update is:

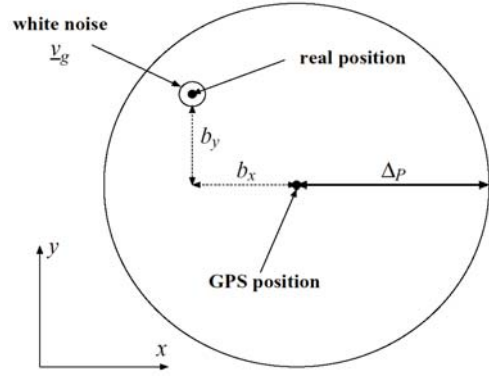$$\underline{X}_{gps} = \underline{X}_{a_k} + \underline{b} + \underline{v}_g , \tag{4}$$

where $X_{gps} = (x_{gps}, y_{gps})^t$ is the vehicle coordinates provided by the GPS, $\underline{v}_g$ and $\underline{b}$ are the parameters included in the model of the GPS data.

This model has white noise $\underline{v}_g$ and could be treated by the Kalman filter. The bias vector $\underline{b}$ will be integrated in the state vector in order to be estimated at the same time as the parameters $x$, $y$, $\gamma$. This bias will be supposed constant from one iteration to another one to ensure convergence of Kalman filter, but this constant evolution model will called into question to each detected fluctuation of the bias (Section 4.2.).

### 2.3. New state vector

Integrating the bias parameters, the new state vector called $\underline{X}$ is:

$$\underline{X} = (\underline{X}_a, b_x, b_y)^t = (x, y, \gamma, b_x, b_y)^t \tag{5}$$

with:
- $x$ and $y$; the vehicle position coordinates in the world reference,
- $\gamma$; the vehicle orientation around the $z$ axis,
- $b_x$ and $b_y$; bias on the $x$ and $y$ axis related to GPS measurements.

The new covariance matrix **Q** associated with this state vector $\underline{X}$ is defined such as :

$$\mathbf{Q} = \begin{pmatrix} \mathbf{Q}_a & \mathbf{Q}_{ab} \\ \mathbf{Q}_{ba} & \mathbf{Q}_b \end{pmatrix}$$

$$= \begin{pmatrix} \sigma_x^2 & \sigma_{xy} & \sigma_{x\gamma} & \sigma_{xb_x} & \sigma_{xb_y} \\ \sigma_{yx} & \sigma_y^2 & \sigma_{y\gamma} & \sigma_{yb_x} & \sigma_{yb_y} \\ \sigma_{\gamma x} & \sigma_{\gamma y} & \sigma_\gamma^2 & \sigma_{\gamma b_x} & \sigma_{\gamma b_y} \\ \sigma_{b_x x} & \sigma_{b_x y} & \sigma_{b_x \gamma} & \sigma_{b_x}^2 & \sigma_{b_x b_y} \\ \sigma_{b_y x} & \sigma_{b_y y} & \sigma_{b_y \gamma} & \sigma_{b_y b_x} & \sigma_{b_y}^2 \end{pmatrix} \tag{6}$$

with $\mathbf{Q}_a$ the covariance matrix with the vehicle attitude defined in Section 1.3. and $\mathbf{Q}_b$ the covariance matrix associated with the bias.

## 2.4. State update
### 2.4.1 Model of observation

Once the bias is integrated in the state vector, the observation equation can be written as follow:

$$\underline{X}_{gps} = \mathbf{H}_g \underline{X}_k + \underline{v}_g \tag{7}$$

with:

$$\mathbf{H}_g = \begin{pmatrix} 1 & 0 & 0 & 1 & 0 \\ 0 & 1 & 0 & 0 & 1 \end{pmatrix}. \tag{8}$$

The covariance matrix associated with $\underline{X}_{gps}$ is:

$$\mathbf{Q}_{gps} = \begin{pmatrix} \sigma^2_{v_{g_x}} & 0 \\ 0 & \sigma^2_{v_{g_y}} \end{pmatrix}, \tag{9}$$

where $\sigma_{v_{g_x}}$ and $\sigma_{v_{g_y}}$ are the standard deviations of the bias coordinate (not of the GPS position coordinates). Their values are about $10cm$.

At the first GPS observation, the bias values ($b_x$ and $b_y$) will be considered as null and the sub-matrix $\mathbf{Q}_b$ representing the covariance matrix of the bias will be initialized with the covariance matrix $\mathbf{Q}i_b$ given by:

$$\mathbf{Q}i_b = \begin{pmatrix} \Delta_P^2 & 0 \\ 0 & \Delta_P^2 \end{pmatrix} \text{ with } \Delta_P = EURE * GDOP. \tag{10}$$

### 2.4.2 Update

Update is realized by Kalman filtering and is described by the following equations:

$$\begin{cases} \underline{X}_{k+1} &= \underline{X}_k &+ \mathbf{K}_g(\underline{X}_{gps} - \mathbf{H}_g \underline{X}_k) \\ \mathbf{Q}_{k+1} &= \mathbf{Q}_k &+ (1 - \mathbf{K}_g \mathbf{H}_g)\mathbf{Q}_k \end{cases} \tag{11}$$

with $\mathbf{K}_g = \mathbf{Q}_k \mathbf{H}_g^t [\mathbf{H}_g \mathbf{Q}_k \mathbf{H}_g^t + \mathbf{Q}_{gps}]^{-1}$

- $\underline{X}_{k+1}$ is the result of the update.
- $\mathbf{Q}_{k+1}$ is the covariance matrix associated with the state vector $\underline{X}_{k+1}$,
- $\mathbf{K}_g$ is the blending factor.

This filter updates the vehicle's attitude and correlates

it with bias parameters, in order to prepare its estimation with incoming exteroceptive information. If no other exteroceptive information is provided by the system, then the bias cannot be estimated and the vehicle position is provided only by the GPS.

Moreover, bias is considered as constant for each update of the state vector, but as explained in Section 2.2. it may not be the case. Therefore, before each update, a possible variation of the bias must be checked. On the contrary all the parameters associated with bias in state vector and in covariance matrix $\mathbf{Q}$ will be reinitialized (see Section 4.2.).

## 3. STATE UPDATE BY VISION DATA

As considered previously, the update of the state vector by other exteroceptive data must allow the estimation of the bias and consequently of the real position of the vehicle. So we propose to use a vision based road-tracker algorithm, giving information on vehicle position and orientation on the roadway to feed the update. This information depends on the vehicle position on the road. The numerical map is necessary to convert this information in the world coordinates system.

### 3.1. Numerical map
#### 3.1.1 Map modeling

The map is constituted by a grid of rectangular areas (Fig. 5) called facets representing the roadsides (actually the white lines of the road). The four points are assumed to be coplanar even if it is not rigorously the case. Finally, the origin of each facet reference frame is situated on the left roadside.

For each facet $i$ five informations are available:

- an identifier (here, a number)
- its position in the world reference frame represented by vector $\underline{O}_i$
- its orientation given by the matrix $\mathbf{R}_i$
- its length $l_i$
- its width $w_i$

The vector $\underline{O}_i$ and the matrix $\mathbf{R}_i$ are defined like this:

$$\underline{O}_i = \begin{pmatrix} x_i \\ y_i \\ z_i \end{pmatrix} \text{ and } \mathbf{R}_i = \begin{pmatrix} X_{i_x} & Y_{i_x} & Z_{i_x} \\ X_{i_y} & Y_{i_y} & Z_{i_y} \\ X_{i_z} & Y_{i_z} & Z_{i_z} \end{pmatrix}. \tag{12}$$

Matrix $\mathbf{R}_i$ represents the orientation of the facet $i$ reference frame such as axis $\underline{Y}_i$ is always in the direction of the vehicle motion on the road.
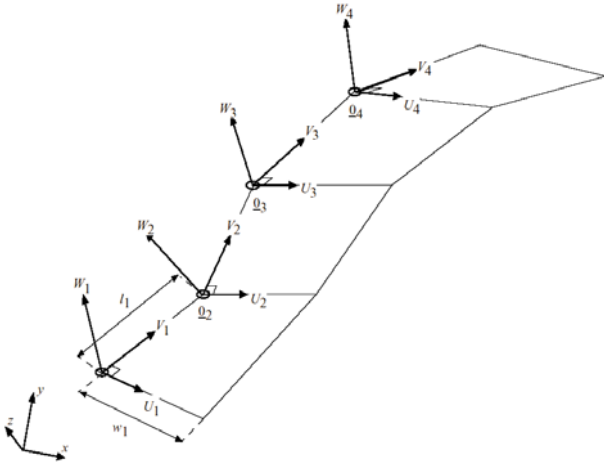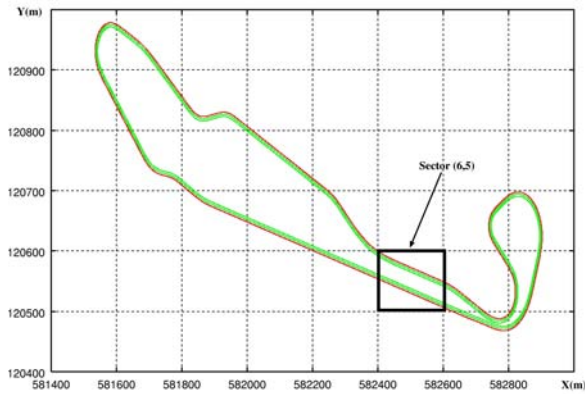
Fig. 5. Road 3D model.



Fig. 6. Map example (military circuit of Satory near Versailles in France).

### 3.1.2 Map organization

When the map becomes very wide, the management of the facets becomes very time expensive. To decrease this complexity, the map is split in several sectors inside which contains a restricted number of facets. So each sector is indexed in the same manner of a two dimensional table inside of which facets are numbered between 1 and $nf$, $nf$ is the total number of facets in the sector. Figs. 6 and 7 show an example of map organization.

### 3.2. Road-tracker algorithm
### 3.2.1 Description

Within our laboratory, a "vision" algorithm able to detect roadsides was developed [2,7] (see Fig. 8). From image primitives representing the roadsides, it allows to estimate with a good precision some parameters describing the road geometry as well as the vehicle position and orientation:

- $L_0$ : the road width,
- $C_0$ : the horizontal road curvature,
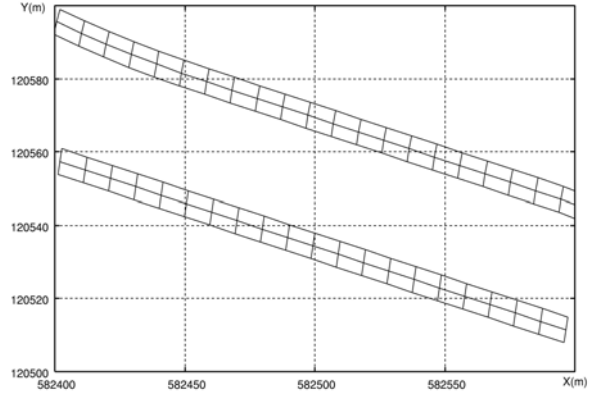- $X_0$ : the lateral position of the vehicle on the road,



Fig. 7. Example of map sector.



Fig. 8. Roadsides detection.

- $\Psi_0$ : the vehicle orientation,
- $\alpha_0$ : inclination angle of the camera.

Also a covariance matrix associated with these parameters is estimated. It should be noticed that all informations are computed in a reference frame tangential with the road (see Fig. 9).

### 3.2.2 Modeling of "vision" information

For the localization of the vehicle on the roadway, only parameters $X_0$ and $\psi_0$ are provided. Information of the longitudinal position is missing. It cannot be estimated by this approach and is considered as null with a very low confidence. Fig. 9 represents each of these parameters with their confidence intervals.

So we can describe "vision" informations by vector $\underline{X}_{vision}$ and its associated covariance matrix $\mathbf{Q}_{vision}$ by :

$$\underline{X}_{vision} = \begin{pmatrix} X_0 \\ \Psi_0 \end{pmatrix} \quad \text{and}$$

$$\mathbf{Q}_{vision} = \begin{pmatrix} \sigma_{X_0}^2 & \sigma_{X_0\Psi_0} \\ \sigma_{\Psi_0 X_0} & \sigma_{\Psi_0}^2 \end{pmatrix}. \tag{13}$$
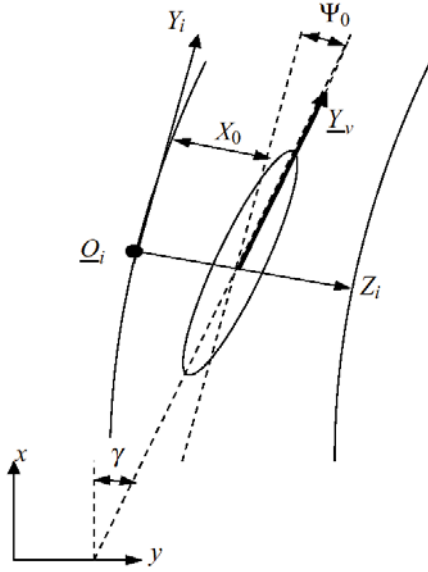
Fig. 9. "Vision" informations.

## 3.3. "Vision"/map coupling

Information given by the road-tracker algorithm has a local meaning (in the road reference frame). "Vision"/map coupling allows to calculate these parameters in the world reference frame. As shown in Section 3.2., information given by "vision" is referred to the left roadside. Which can be considered as the reference frame described by the orientation matrix $\mathbf{R}_i$ associated with the facet carrying the vehicle.

Three stages are necessary to calculate "vision" information into the world reference frame: (1) the facet on which the vehicle is located or the nearest one is searched, (2) vehicle position in facet reference frame is computed and (3) the vehicle position and orientation are converted in the world reference frame.

### 3.3.1 Facet search

Initially, the map sector where the vehicle is positioned is found. Then, all the facets contained in this sector having a contrary direction with the road circulation wise are eliminated. Finally only the facet where the vehicle is, or the nearest one is selected. The next paragraph details the facet search.

**Facet elimination**

At any moment, the vehicle direction can be described by the following vector (see Fig. 9):

$$\underline{Y}_v = \mathbf{R}_\gamma \begin{pmatrix} 0 \\ 1 \\ 0 \end{pmatrix} \tag{14}$$

with:

$$\mathbf{R}_\gamma = \begin{pmatrix} cos(\gamma) & -sin(\gamma) & 0 \\ sin(\gamma) & cos(\gamma) & 0 \\ 0 & 0 & 1 \end{pmatrix} \tag{15}$$

and $\gamma$ is the vehicle orientation in the world reference frame.

For each facet $i$, the road direction wise is described by the vector $\underline{Y}_i$ deduced from the orientation matrix $\mathbf{R}_i$ of the considered facet. Therefore, the direction compatibility between the facet direction and the vehicle direction is given by a test on the next scalar product:

$$D_{f/v} = \underline{Y}_i \cdot \underline{Y}_v . \tag{16}$$

If the scalar product is lower than 0, then the vehicle orientation is not compatible with the road direction and the vehicle cannot be located.

**Facet determination**

For each remaining facet, vehicle position in the facet reference frame is computed by a matrix product. Using the notation defined in (12), the vehicle position is given by the following equations:

$$\begin{pmatrix} X \\ Y \end{pmatrix} = \begin{pmatrix} X_{i_x} & Y_{i_x} \\ X_{i_y} & Y_{i_y} \end{pmatrix} \begin{pmatrix} x - x_i \\ y - y_i \end{pmatrix} . \tag{17}$$

If $0 < X < w_i$ and $0 < Y < l_i$, the vehicle is located on the facet $i$ and the research is stopped. If not, the distance between the facet origin $O_i$ and the vehicle position is computed in the facet reference frame. Finally if the vehicle is not positioned on any facet in the map sector, the nearest one to the vehicle is selected.

Now, the facet $i$ of the road map supposed to carry the vehicle is known, it is possible to convert local attitude provided by the road-tracker algorithm in the world reference frame before update.

### 3.3.2 Transformation from facet reference frame to world reference frame

**Attitude vector**

The transformation from vehicle attitude $(X, Y, \Psi)^t$ in the reference frame of the facet $i$ to the world reference frame is described by the following relations:

$$x = X_{i_x} X + Y_{i_x} Y + x_i ,$$
$$y = X_{i_y} X + Y_{i_y} Y + y_i , \tag{18}$$
$$\gamma = \Psi - atan(\frac{Y_{i_x}}{Y_{i_y}}) .$$

Considering a flat world, the transformation equations of attitude vector $\underline{X}_{vision} = (X_0, 0, \Psi_0)^t$ given by the

"vision" system (see Section 3.2.) into the world reference frame can be deduced. The resulting vector is named $\underline{X}_{vision/m}$.

$$\underline{X}_{vision/m} = \begin{pmatrix} X_{i_x} X_0 + x_i \\ X_{i_y} X_0 + y_i \\ \Psi_0 - atan(\dfrac{Y_{i_x}}{Y_{i_y}}) \end{pmatrix} \qquad (19)$$

**Associated covariance matrix**

To deduce the covariance matrix associated with vector $\underline{X}_{vision/m}$, it is necessary to take into account the possible dispersion of "vision" information. Indeed this one does not provide only one vehicle position but a set of positions which are contained in the ellipsoid deduced from the covariance matrix $\mathbf{Q}_a$. Fig. 10 describes an example of the possible positions $X_j$ and $Y_j$ in the reference frame of facet $i$ for a given vehicle attitude.

We can see in Fig. 10 that the possible positions have the same trajectory as the roadsides. As shown in [2] a road can be locally modeled by a parabola. The road-tracker algorithm provides the road curvature $C_0$ and consequently vehicle positions on the roadway can be modeled by the following equations :

$$\begin{cases} X_j = \dfrac{C_0}{2} Y_j^2 + X_0 \\ Y_j \\ \Psi_j = C_0 Y_j + \Psi_0. \end{cases} \qquad (20)$$
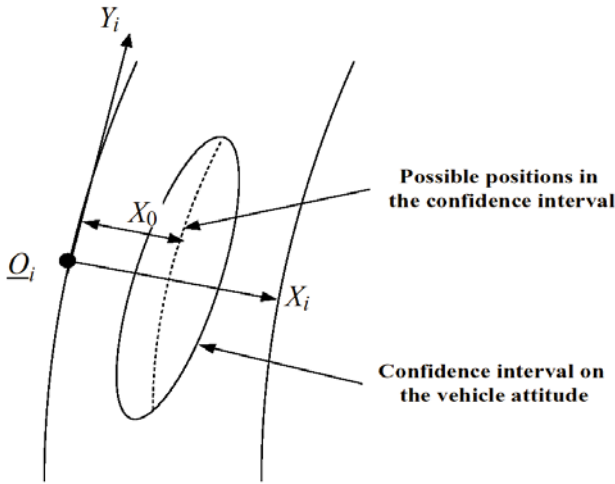


Fig. 10. Possible positions given by the "vision" algorithm.

If we consider that $Y_j$ fluctuates around $Y \pm \Delta_y$ (with $\Delta_y$ the value of the large axis $y$ of the ellipsoid described by the covariance matrix $\mathbf{Q}_a$) then all of the vehicle positions can be computed and covariance matrix associated with the vector $\underline{X}_{vision/f}$ can be deduced by the following equations:

$$\mathbf{Q}_{vision/f} = 1/N \sum_{i=1:N} \begin{pmatrix} X_j - X \\ Y_j - Y \\ \Psi_i - \Psi \end{pmatrix} \begin{pmatrix} X_j - X \\ Y_j - Y \\ \Psi_j - \Psi \end{pmatrix}^t \qquad (21)$$
$$+ \mathbf{M}_v \mathbf{Q}_{vision} \mathbf{M}_v^t$$

with:

$$\mathbf{M}_v = \begin{pmatrix} 1 & 0 \\ 0 & 0 \\ 0 & 1 \end{pmatrix}. \qquad (22)$$

Finally the covariance matrix $\mathbf{Q}_{vision/m}$ associated with the vector $\underline{X}_{vision/m}$ in the world reference frame is:

$$\mathbf{Q}_{vision/m} = \mathbf{M}_p \mathbf{Q}_{vision/f} \mathbf{M}_p^t \qquad (23)$$

with:

$$\mathbf{M}_p = \begin{pmatrix} X_{i_x} & Y_{i_x} & 0 \\ X_{i_y} & Y_{i_y} & 0 \\ 0 & 0 & 1 \end{pmatrix}. \qquad (24)$$

3.4. State update

3.4.1 Model of observation

The model of observation for "vision" data is described by the following equation:

$$\underline{X}_{vision/m} = \mathbf{H}_v \underline{X}_k + \underline{v}_v \qquad (25)$$

with:

$$\mathbf{H}_v = \begin{pmatrix} 1 & 0 & 0 & 0 & 0 \\ 0 & 1 & 0 & 0 & 0 \\ 0 & 0 & 1 & 0 & 0 \end{pmatrix}. \qquad (26)$$

The variance of the noise $\underline{v}_v$ is modeled by covariance matrix $\mathbf{Q}_{vision/m}$.

3.4.2 Update

In the same way as for GPS, the state update is realized by a Kalman filter:

$$\begin{cases} \underline{X}_{k+1} = \underline{X}_k + \mathbf{K}_v(\underline{X}_{vision} - \mathbf{H}_v \underline{X}_k) \\ \mathbf{Q}_{k+1} = \mathbf{Q}_k + (1 - \mathbf{K}_v \mathbf{H}_v)\mathbf{Q}_k \end{cases} \qquad (27)$$

with    $\mathbf{K}_v = \mathbf{Q}_k \mathbf{H}_v^t [\mathbf{H}_v \mathbf{Q}_k \mathbf{H}_v^t + \mathbf{Q}_{vision}]^{-1}$

- $\underline{X}_{k+1}$ is the result of the update,
- $\mathbf{Q}_{k+1}$ is new covariance matrix associated with state vector,
- $\mathbf{K}_v$ is the blending factor.

## 4. PREDICTION STAGE

### 4.1. Prediction of the state vector

The evolution model allows to write the recurrent relation between state vectors $\underline{X}_{k+1}$ and at time $k+1$ according to its value $\underline{X}_k$ and to parameters provided by the proprioceptive sensors at time $k$. This information is the wheel angle $\delta$ and the traveled distance of the vehicle $\Delta_d$ between time $k$ and time $k+1$.

$$\underline{X}_{k+1} = f(\underline{X}_k, \underline{U}_k) \quad \text{with} \quad \underline{U}_k = (\Delta_d, \delta) \qquad (28)$$

The model used, is a bicycle model (Fig. 11).
The new vehicle position $(x,y)_{k+1}$ can be defined according to $(x,y)_k$, knowing $\Delta_d$ and $\delta$.

$$\begin{pmatrix} x_{k+1} \\ y_{k+1} \end{pmatrix} = \begin{pmatrix} x_k \\ y_k \end{pmatrix} + \begin{pmatrix} cos(\gamma_k + \delta) & -sin(\gamma_k + \delta) \\ sin(\gamma_k + \delta) & cos(\gamma_k + \delta) \end{pmatrix} \begin{pmatrix} 0 \\ \Delta_d \end{pmatrix} \quad (29)$$

therefore:

$$\begin{cases} x_{k+1} = x_k - \Delta_d sin(\gamma_k + \delta) \\ y_{k+1} = y_k + \Delta_d cos(\gamma_k + \delta). \end{cases} \qquad (30)$$

The new vehicle orientation $\gamma_{k+1}$ is given by the following equation:

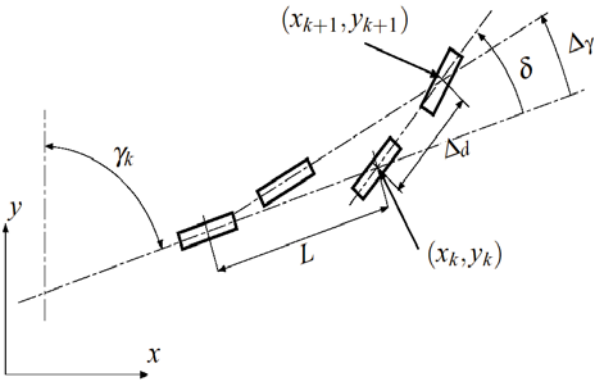$$\gamma_{k+1} = \gamma_k + \Delta_\gamma \qquad (31)$$



Fig. 11. Bicycle model.

with:

$$\Delta_\gamma = \arctan \frac{\Delta_d sin(\delta)}{L + \Delta_d cos(\delta)} . \qquad (32)$$

Finally, no evolution on the bias is computed because it is considered as constant between two GPS data (see Section 2.2.).

Considering (30) and (31), the evolution of the state vector can be written like this:

$$\begin{cases} x_{k+1} = x_k - \Delta_d \sin(\gamma_k + \delta) \\ y_{k+1} = y_k + \Delta_d \cos(\gamma_k + \delta) \\ \gamma_{k+1} = \gamma_k + \Delta_{\gamma_k} \\ b_{x_{k+1}} = b_{x_k} \\ b_{y_{k+1}} = b_{y_k} \end{cases} \qquad (33)$$

And the new covariance matrix associated with the state vector can be deduced from the following equations:

$$\mathbf{Q}_{k+1} = \mathbf{J}_e \mathbf{C}_e \mathbf{J}_e^t, \qquad (34)$$

where $\mathbf{C}_e$ is a covariance matrix constituted by $\mathbf{Q}_k$ and $\mathbf{Q}_{U_k}$ associated with the entries vector $\underline{U}_k = (\Delta_d, \delta)$. And $\mathbf{J}_e$ is the Jacobian matrix deduced from the evolution equations.

$$\mathbf{C}_e = \begin{pmatrix} \mathbf{Q}_k & 0 \\ 0 & \mathbf{Q}_{U_k} \end{pmatrix} \quad \text{with} \quad \mathbf{Q}_{U_k} = \begin{pmatrix} \sigma_{\Delta_d}^2 & 0 \\ 0 & \sigma_\delta^2 \end{pmatrix} \quad (35)$$

and

$$\mathbf{J}_e = \frac{\partial \underline{X}_{k+1}}{\partial(x_k, y_k, \gamma_k, \Delta_d, \delta)}$$

$$= \begin{pmatrix} 1 & 0 & -\Delta_d C\gamma\delta & 0 & 0 & -S\gamma\delta & -\Delta_d S\gamma\delta \\ 0 & 1 & -\Delta_d S\gamma\delta & 0 & 0 & C\gamma\delta & -\Delta_d C\gamma\delta \\ 0 & 0 & 1 & 0 & 0 & \frac{\partial \Delta_\gamma}{\partial \Delta_d} & \frac{\partial \Delta_\gamma}{\partial \Delta_d} \\ 0 & 0 & 0 & 1 & 0 & 0 & 0 \\ 0 & 0 & 0 & 0 & 1 & 0 & 0 \end{pmatrix} \quad (36)$$

with:

$$\begin{aligned} S\gamma\delta &= sin(\gamma_k + \delta), \\ C\gamma\delta &= cos(\gamma_k + \delta). \end{aligned} \qquad (37)$$

Fig. 12 shows the displacement of the vehicle between time $k$ and time $k+1$ and the confidence intervals on the vehicle position.

## 4.2. GPS prediction and bias management
### 4.2.1 Prediction of the new GPS position

As it was explained in Section 4.2. the bias is assumed as constant from one iteration to another one, but it can fluctuate at any moment. Therefore it's necessary to compare the prediction of the new GPS position with the real GPS position to detect variations of this one before using GPS data to update the bias.

If the bias is considered as constant between two GPS data, trajectory of GPS positions must be parallel to vehicle trajectory and GPS positions displacement is the same ones of the vehicle displacement. So, considering (30), for any new proprioceptive data, the new GPS position can be predicted like this:

$$x_{gps_{k+1}} = x_{gps_k} - \Delta_d sin(\gamma_k + \delta),$$
$$y_{gps_{k+1}} = y_{gps_k} + \Delta_d cos(\gamma_k + \delta).$$
(38)

The new covariance matrix associated with the GPS position is given by the next relation:

$$\mathbf{Q}_{gpsk+1} = \mathbf{J}_g \mathbf{C}_g \mathbf{J}_g^t,$$
(39)

where $\mathbf{C}_g$ is a covariance matrix constituted by the covariance matrix $\mathbf{Q}_{gps_k}$ and the covariance matrix $\mathbf{Q}_{U_k}$ associated with the entries vector $\underline{U}_k$. And $\mathbf{J}_g$ is the Jacobian matrix deduced from the evolution equations of the new GPS position.

$$\mathbf{C}_g = \begin{pmatrix} \mathbf{Q}_{gps_k} & 0 \\ 0 & \mathbf{Q}_{U_k} \end{pmatrix}$$
(40)

and

$$\mathbf{J}_g = \frac{\partial \underline{X}_{gps_{k+1}}}{\partial(x_k, y_k, \Delta_d, \delta)}$$
(41)
$$= \begin{pmatrix} 1 & 0 & -S\gamma\delta & -\Delta_d S\gamma\delta \\ 0 & 1 & C\gamma\delta & -\Delta_d C\gamma\delta \end{pmatrix}.$$

### 4.2.2 Bias management

In order to check that the bias has not changed from an iteration to an another one, it's necessary for the GPS position to be contained in the confidence interval (see Fig. 13) described by the vector $\underline{X}_{gps_{k+1}}$ and the covariance matrix $\mathbf{Q}_{gps_{k+1}}$. This new confidence interval is computed from the last $\underline{X}_{gps}$ and $\mathbf{Q}_{gps}$ provided by the GPS as well as the proprioceptive informations (see Section 4.2.).

To test if the GPS position remains within the confidence interval, the following Mahalanobis distance is computed:
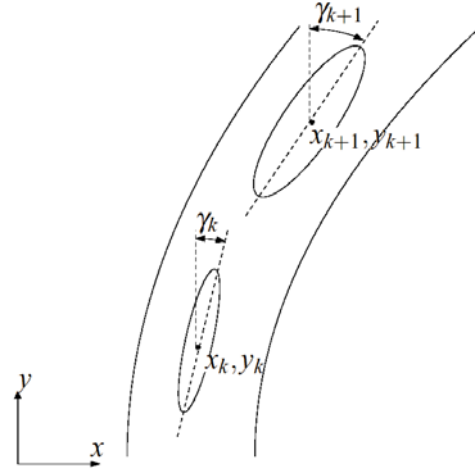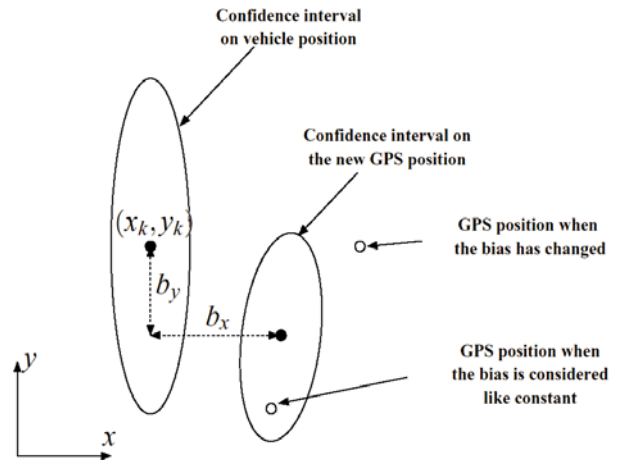


Fig. 12. Vehicle evolution.



Fig. 13. Bias variations.

$$d = (\underline{X}_{gps} - \underline{X}_{gps_{k+1}})\mathbf{Q}_{gps_{k+1}}^{-1}(\underline{X}_{gps} - \underline{X}_{gps_{k+1}})^t \quad (42)$$

$d < 1$ means the GPS point is situated inside the uncertainty ellipsis corresponding to one standard deviation. The experiments show this condition is sufficient to insure that the bias has not changed. Then the bias can be updated. $d > 1$ means the bias was subject to a strong variation. The reinitialization of the covariance matrix associated with state vector and bias parameters in the state vector is needed before the update. For this: $\mathbf{Q}_b$ will take its initial value ($\mathbf{Q}i_b$ see (10)) and covariance between the vehicle attitude parameters and bias parameters are set to zero. Then using (6), $\mathbf{Q}_k$ becomes:

$$\mathbf{Q}_k = \begin{pmatrix} \sigma_x^2 & \sigma_{xy} & \sigma_{x\gamma} & \\ \sigma_{yx} & \sigma_y^2 & \sigma_{y\gamma} & 0 \\ \sigma_{\gamma x} & \sigma_{\gamma y} & \sigma_\gamma^2 & \\ & 0 & & \mathbf{Q}i_b \end{pmatrix}.$$
(43)

Having no knowledge about the new value of the bias, it is considered as the difference between the estimate position of the vehicle in the state vector and the new position provided by the GPS in according with the confidence interval given by the constructor. So, the bias can be described by the following equations:

$$b_{x_k} = x_k - x_{gps}$$
$$b_{y_k} = y_k - y_{gps}$$    (44)

with:

$$0 <| b_{x_k} |< \Delta_P$$
$$0 <| b_{y_k} |< \Delta_P.$$    (45)

If the above relation are not respected then $b_{x_k}$ and $b_{y_k}$ are sat to zero.

## 5. LOCALIZATION RESULTS

In this section we present the experimental results obtained on an avenue near the middle of Clermont-Ferrand. This experimental travel presents several kind of road contexts: 2x2 lanes, 1x1 lane and a traffic circle (see Fig. 14).

Results are presented in three parts:

- the first one presents the behavior of the system when the GPS signal is lost,
- the second one describes the localization results when the bias fluctuates,
- and the last one shows the precision obtained with this system.

Before the presentation of these results, the experimental framework is detailed.

### 5.1. Experimental framework

The tests have been realized using an experimental vehicle. This is a Citroën Evasion equipped (Fig. 15) with several devices :
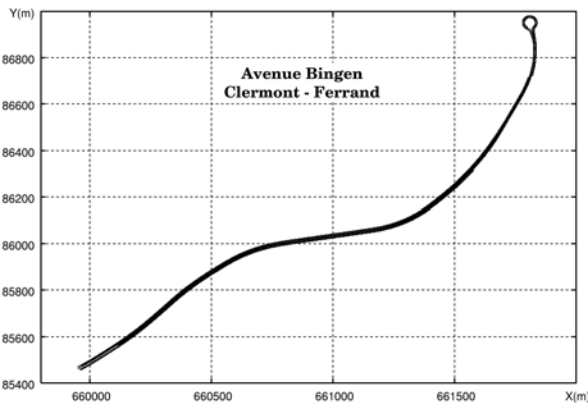


Fig. 14. Map of bingen avenue.
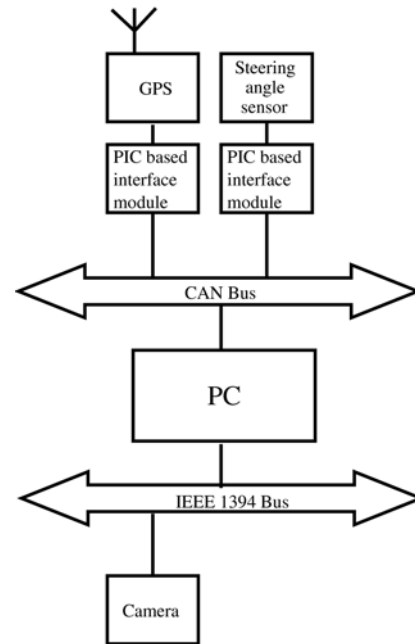


Fig. 15. Experimental vehicle used.



Fig. 16. Data acquisition architecture.

- a steering angle sensor which is simply a standard potentiometer coupled with the steering wheel axis,
- a low cost GPS similar to the one used for commercial vehicle guidance systems,
- a video camera installed inside the car near the rear view mirror and looking at the road in front of the vehicle,
- an on boarded PC for sensor data acquisition, image processing and localization computation.

The data acquisition is managed by a specific software able to recover the data on several kinds of interface busses (CAN bus, IEEE 1394 bus) within a hardware architecture illustrated Fig. 16 and to insert each one onto a time scale using a dating and synchronism process of our own which is not described here.

The time intervals between sensing points is not constant but as soon as the corresponding data are

correctly positioned on the time scale this interval is well known and can be used for the localization.

The position updating is achieved each time a sensor data arrives with its correct dating, using the corresponding Kalman filter equation as explained in the previous sections.

5.2. Behavior when GPS signal is lost

In this first part, we will show the reactions of the localization system in the case of GPS signal losses. This situation is rather frequent in urban environments. In order to show the robustness of our approach, we have simulated a loss of GPS signal between $15s$ and $30s$ in two different cases: with and without "vision" informations (see Fig. 17).

Fig. 17(a) is the result of the localization without "vision" information and without loss of GPS signal: the system provides an approximate trajectory of the vehicle. This first one passes through all GPS position because the system is not able to estimate the bias without "vision" (see Section 2.4.).

Figs. 17(b) and 17(c) are the localization results without "vision" and with losses of GPS signal going from $15s$ to $30s$. The longer the loss of GPS signal is, the higher the difference of the position in comparison with the result in the first graphic (like statement in Section 1.1.).

Finally, the Fig. 17(d) shows the localization results when "vision" is enabled. It can be noticed that despite the loss of GPS signal, the system provides a correct position. The vehicle trajectory does not pass through the GPS positions, because the system is able to estimate the bias thanks to the "vision" data.

As it's shown in Fig. 17(d), the use of "vision" data associated with a numerical map of road network allows to provide a good estimation of the vehicle position even if the GPS data are not present. So, this is very interesting in urban or tunnel situations. If we assume that map errors are insignificant, the precision obtained in the estimated localization strongly depends on the precision of the road-tracker algorithm.

5.3. Bias variations

Now the behavior of the system when the bias changes suddenly is presented. Fig. 18 (18(a) to 18(f)) show the localization results, positions provided by the GPS, the estimate of the GPS position and its confidence interval on the map for each update by GPS data. Table 2 presents some corresponding numerical values as well as the value of the Mahalanobis distance (see Section 2.4) during the update.

At time $t = t_0$ the system provides an estimation of the vehicle position and a bias estimation called $b_0$, this one was learned by the system during several preceding iterations.

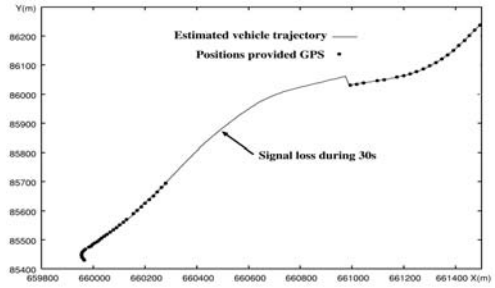Table 2. Numerical results of bias variations.

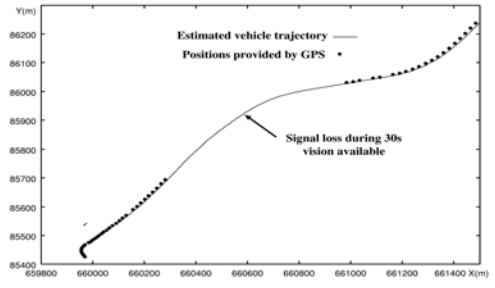| t | Measured bias (m) | | Estimated bias (m) | | Malahanobis Distance |
|---|---|---|---|---|---|
| $t_0$ | 2.43 | 3.71 | 2.43 | 3.76 | 0.04 |
| $t_1$ | 28.11 | 7.53 | 2.62 | 3.72 | 8924.36 |
| $t'_1$ | 28.09 | 7.54 | 28.09 | 7.54 | None |
| $t_2$ | 2.46 | 3.64 | 27.88 | 7.54 | 8887.61 |
| $t'_2$ | 2.45 | 3.63 | 2.45 | 3.63 | none |
| $t_3$ | 2.31 | 3.74 | 2.44 | 3.68 | 0.65 |
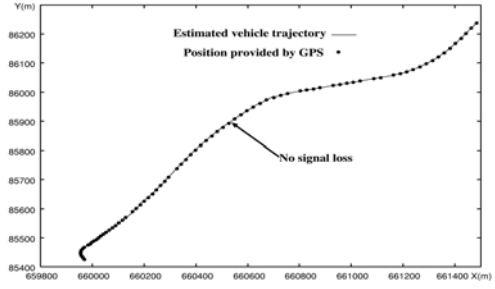


(a)
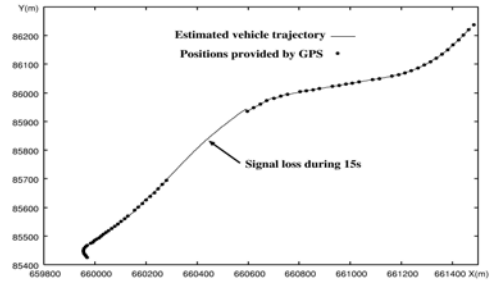


(b)



(c)



(d)

Fig. 17. Vehicle localization : (a) no signal loss, vision not available, (b) signal loss during 15s and vision not available, (c) signal loss during 30s and vision not available, (d) signal loss during 30s and vision available.
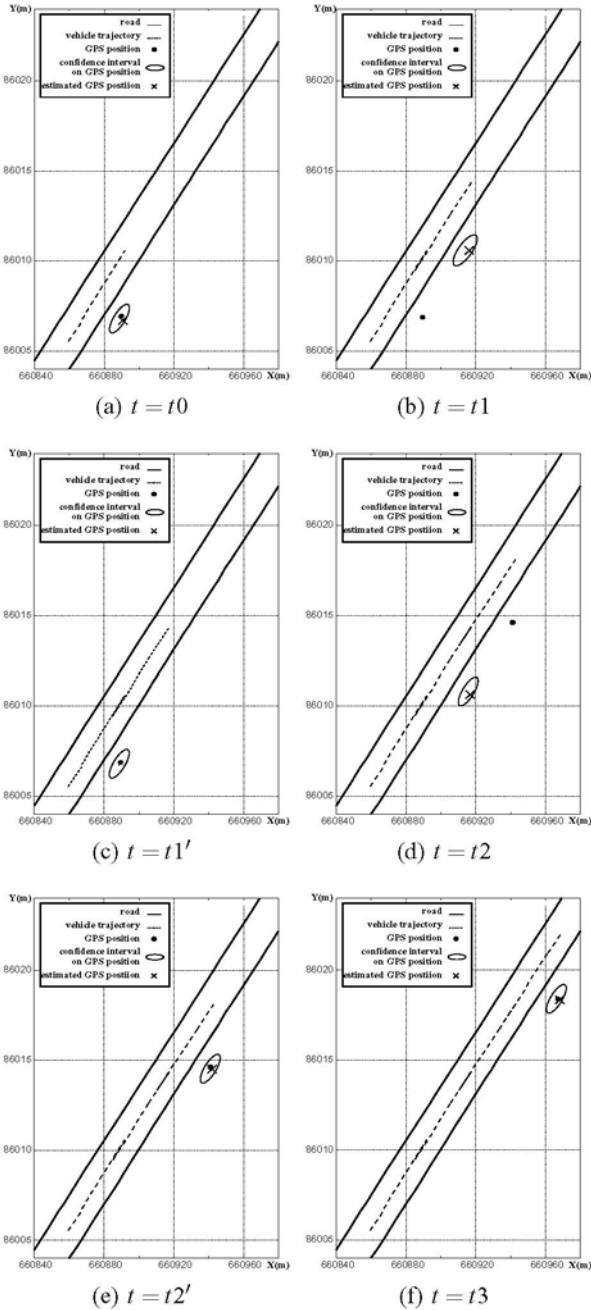
Fig. 18. Bias behavior at different times.

At time $t = t_1$ a bias variation happens. Estimations of GPS position is false and the GPS position is out of the confidence interval (Mahalanobis distance $d = 8924.36 > 1$), this one has been computed in the meantime of the prediction of the new GPS position. After the update (at time $t = t'_1$) we can see that the new estimation of the GPS position is the same that the GPS position indeed the bias was re-initialized. Regarding estimation of the vehicle position, this one has varied only of few centimeters between $t_1$ and $t'_1$, therefore the update has no influence on the vehicle position estimations.

At time $t = t_2$, GPS data are skewed again by a bias close to $b_0$ ( $d = 8887.61$ ). We are in the same situation at time $t = t_1$ et $t = t'_1$. According to the results obtained at time $t = t'_2$ the system reacts in the same way, bias is initialized and the update has no influence on the estimation of the vehicle position.

Finally at time $t = t_3$ the bias is correctly estimated, as shown by the Mahalanobis distance $d = 0.65$. The update is realized without bias re-initialization.

So, according to these results, the system is appropriate to manage GPS data uncertainties (change of visibility of the satellites or multi-path interferences) and it allows to estimate a good vehicle position even if the bias is subject to some variations.

5.4. Precision obtained by the system

Initially we present the precision obtained in motor-way situations (2x2 lanes). Four situations will be described: the initialization step, a second one where "vision" information is available, a third one with a loss of GPS signal and a last situation where all sensor data are available (Fig. 19). For a better comprehension, all the results are given in the road reference frame: lateral position and orientation of the vehicle on the roadway.
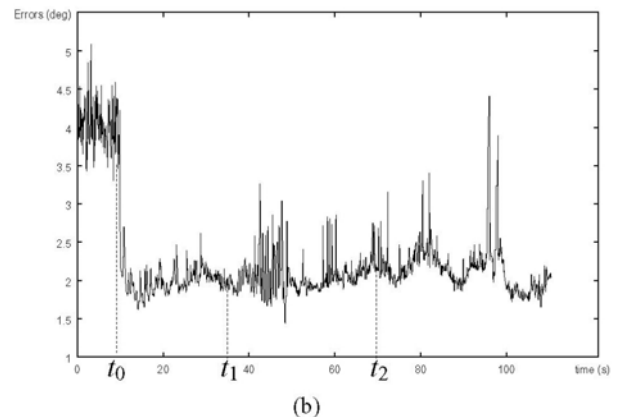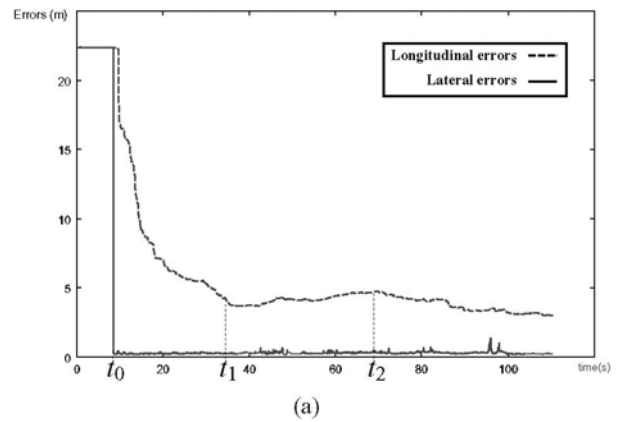


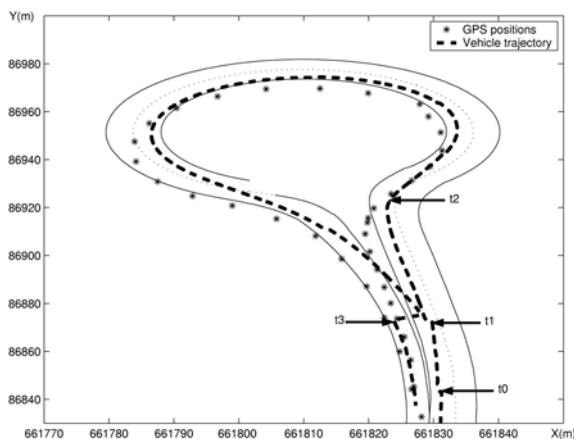Fig. 19. Localization uncertainties : (a) position, (b) orientation.

Fig. 20. Vehicle trajectory in the traffic circle.

Between time $t = 0$ and $t = t_0$ the state is only updated by GPS data and the prediction by proprioceptive sensors ("vision" data are not taken into account). The system allows to know an approximated position and orientation of the vehicle, uncertainties on the lateral position and longitudinal position are about 30m (corresponding to $\Delta_p$ defined 2.2.). Uncertainty of orientation angle $\Psi$ is about 4 degrees with fluctuation of 1 degree due to uncertainties on the proprioceptive sensor data.

From time $t_0$ to $t_1$ the update by "vision" data is available, uncertainties on the lateral position of the vehicle decreases to $20cm$, on the longitudinal position to $4m$ and on the orientation angle $\Psi$ to about 2 degrees.

From time $t_1$ to $t_2$ the loss of the GPS signal have no influence on the localization results. Rather high variations on the orientation angle are visible, they are due to lane change or to a bad recognition of the road by the "vision" algorithm.

Finally after time $t_2$ the localization is refined while the road-tracker provides good informations.

Now we will show the precision obtained when the road-tracker algorithm is not able to provide good information to the localization system. An example of traffic circle will be described (see Fig. 20). The experimentation is as follow: after having covered $2km$ (at time $t = t_0$) the vehicle is localized with a good precision, it arrives to a traffic circle by the left lane of a 2x2 lanes way, goes around the traffic circle and goes out in opposite direction of the 2x2 lanes. The estimations of the vehicle trajectory and GPS position are described respectively by dashed layout and stars.

At time $t = t_0$ and $t = t_1$ the road tracker makes a poor estimation of the vehicle attitude involving a poor localization of the vehicle in the world. Afterwards the "vision" algorithm does not provide an information. The estimated trajectory remains rather

good due to the proprioceptive sensors and regardless the uncertainty of GPS information.

From time $t = t_2$ to $t = t_3$ the road-tracker algorithm is not able to provide good information in traffic circle context, therefore "vision" is not available and only GPS information is used to update the state vector. The trajectory provided by the system follows the traffic circle but when the vehicle leaves this, the estimated position is not on the correct lane because of the drift of the proprioceptive sensors. The precision of each parameter decreases according to the traveled distance.

At time $t >= t_3$ "vision" is available again, the vehicle is positioned on the correct lane and precision onto the parameters have similar values as at time $t = t_0$.

According to these results, the localization precision strongly depends on "vision" information. If road-tracker does not provide any information then the localization precision decreases but remains higher than the precision of the GPS alone.

## 6. CONCLUSION

This article present a low cost method both precise and robust for vehicle localization in road network. Taking into account of the bias on the GPS data into the state vector allows the localization system to be insensitive to losses of GPS data as well as of variations due to satellites visibility. Original association of a vision algorithm able to provide a precise vehicle localization on the road with a numerical map of the road network allows the localization system to obtain a good accuracy (precision of some $10cm$).

As it is shown in the localization results, no "vehicle on road" hypothesis is taken into account in the localization process, we plan to deal with this problem by using a particle filter and information provided by the numerical map of the road network. This method should manage the multi-assumptions in terms of positioning that we can meet in the situations of 2x2 lanes or in the crossroads. It should avoid the principal drawbacks of Kalman filter (non-linear estimation, nonwhite noises). A second part of our future works is to add a tracking module to the "vision" algorithm by using the data provided by the proprioceptive sensors, thanks to this module we hope to improve road detection, increase the precision of "vision" information vision and by the same opportunity improve the vehicle localization. The overall precision of the localization is at the present time evaluated by a posteriori variances on the estimated vehicle attitude. We plan to use a DGPS system as reference position sensor to compare the position it provides with the estimated one.

## REFERENCES

[1] S. Arulampalam, S. Maskell, N. Gordon, and T. Clapp, "A Tutorial on particle filters for on-line non-linear/non-Gaussian Bayesian tracking," *IEEE Trans. on Signal Processing,* vol. 50, no. 2, pp. 174-188, February 2002.

[2] R. Aufrère, *Reconnaissance et suivi de route par vision artificielle application à l'aide à la conduite,* PhD thesis, Université Blaise Pascal, Clermont-Ferrand, France, 2001.

[3] P. Bonnifait, *Localisation préise en position et attitude des robots mobiles d'extéieur,* PhD thesis, Ecole centrale de Nantes, France, 1997.

[4] J. Borenstein and L.Feng, "Gyrodometry: A new method for combining data from gyros and odometry in mobile robots," *Proc. of the IEEE International Conference on Robotics and Automation,* pp. 423-428, Minneapolis, Minnesota, April 22-28, 1996

[5] S. Botton, F. Duquenne, Y. Egels, M. Even, and P. Willis, GPS *Localisation et Navigation,* Hermes, 1998.

[6] D. Bouvet, *Contribution à la localisation d'engins de chantiers routiers,* PhD thesis, Ecole centrale de Nantes, France, 2000.

[7] R. Chapuis, J. Laneurit, R.Aufrère, F. Chausse, and T. Chateau, "Accurate vision based road tracker," *Proc. of IEEE Int. Conf. on Intelligent Vehicles,* Versailles, France, CD-ROM file no IV-103.pdf, June 18-20, 2002.

[8] M. Chung, L. Ojeda, and J. Borenstein, "Sensor fusion for mobile robot dead-reckoning with a precision-calibrated fiber optic gyroscope," *Proc. of the IEEE International Conference on Robotics and Automation,* pp. 3588-3593, Korea, May 21-26, 2001.

[9] S. Clark, G. Dissanayake, P. Newman, and H. Durrant-White, "A solution to simultaneous localization and map building (SLAM) problem," *International Journal of Robotic and Automation,* vol. 17, no. 3, pp. 229-241, 2001.

[10] P. H. Dana, "Global positioning system (GPS) time dissemination for real-time applications," *International Journal of Time Critical Computing Systems,* vol. 12, no. 1, pp. 9-40, 1997.

[11] C. Durieu, M. J. Aldon, and D. Meizel, "La fusion de données multisensorielles pour la localisation en robotique mobile," *Traitement du signal,* vol. 13, no. 2, pp. 143-166, 1996.

[12] E. Kiriy and M. Buehler, *Three-state Extended Kalman Filter for Mobile Robot Localization,* Technical Report, Electrical and Computer Engineering, McGill University, Montréal, 2002.

[13] M. E. El Najjar and Ph. Bonnifait, "A roadmap matching method for precise vehicle localization using belief theory and Kalman filtering," *Proc. of International Conference on Advanced Robotics,* pp. 1677-1682, Portugal, July 2003.

[14] K. Ohno, T. Tsubouchi, B. Shigematsu, S. Maeyama, and S. Yuta, "Outdoor navigation of a mobile robot between buildings based on DGPS and odometry data fusion," Proc. of *IEEE Int'l Conf. on Robotics and Automation,* pp. 1978-1984, September 14-15, 2003.

[15] C. F. Olson, "Selecting landmarks for localization in natural terrain," *Autonomous Robots Systems,* vol. 12, no. 2, pp. 201-210, March 2002.

[16] L. Pronzato and E. Walte, "Minimal-volume ellipsoids," *International Journal of Adaptive Control and Signal Processing,* vol. 8, no. 2, pp. 15-30, 1994.

[17] I. M. Rekleitis, *Cooperative Localization and Multi-Robot Exploration,* School of Computer Science, McGill University, Montreal, Quebec, Canada, 2003.

[18] U. Scheunert, H. Cramer, and G. Wanielik, "Precise vehicle localization using multiple sensors and natural landmarks," *Proc. of the Seventh International Conference on Information Fusion,* pp. 649-656, Stockholm, Sweden, June, 2004.

[19] F. C. Schweppe, "Recursive state estimation : unknown but bounded errors and system inputs," *IEEE Trans. on Automatic Control,* vol. 13, no. 1, pp. 22-28, 1968.

[20] R. Talluri and J. K. Aggarwal, "Image/map correspondence for mobile robot self-location using computer graphics," *IEEE Trans. on Pattern Analysis and Machine Intelligence,* vol. 15, no. 6, pp. 597-601, June 1993.

[21] R. Thrapp, C. Westbrook, and S. Devika, "Robust localization methods for an autonomous campus tour guide," *Proc. of the International Conference on Robotics and Automation,* Korea, May 21-26, 2001.

[22] S. Thrun, D. Fox, W. Burgard, and F. Dellaert, "Robust monte carlo localization for mobile robots," *Artificial Intelligence*, vol. 128, no. 1-2, pp. 99-141, 2000.

[23] J. Vaganay, J. G. Belligham, and J. Leonard, "Comparison of fix computation and filtering for autonomous acoustic navigation," *Inter-national Journal of Systems Science,* vol. 29, pp. 1111-1122, 1998.

[24] J. Vaganay, *Conception d'un système multisensoriel de localisation dynamique 3D pour robot mobile,* PhD thesis, University Montpellier II, France, 1993.

[25] G. Welch and G. Bishop, *An Introduction to the Kalman Filter,* University of North Carolina, Department of Computer Science, Chapel Hill, NC, USA, TR95-041, 2004.

[26] Y. Cui and S. S. Ge, "Autonomous vehicle

positioning with GPS in urban canyon environments," *IEEE Trans. on Robotics and Automation,* vol. 19, no. 1, pp. 15-25, February 2003.

**Roland Chapuis** is Professor at the University Center Of Sciences and Technics engineer school. He became state doctor in 2000. His research in road scene analysis for driving assistance is conducted at the LASMEA laboratory.

**Jean Laneurit** is Ph.D. Student at the LASMEA-GRAVIR research laboratory of Blaise Pascal University France. His works concerns data fusion for robot localization with an application to on map vehicle positioning for driving assistance.

**Frédéric Chausse** is Associate Professor at the Applied Physics Department of the University Institute of Technology of Auvergne University, France. He received the Ph.D. in 1994. His research works are about image analysis of road scenes.